Cellular Automata Segmentation of the Boundary between the Compacta of Vertebral Bodies and Surrounding Structures

Jan Egger [a,b,c] and Christopher Nimsky [a]

[a] University of Marburg, Dept. of Neurosurgery, Baldingerstr., 35033 Marburg, Germany
[b] TU Graz, Institute for Computer Graphics and Vision, Inffeldgasse 16, 8010 Graz, Austria
[c] BioTechMed, Krenngasse 37/1, 8010 Graz, Austria

Introduction

Due to the aging population, spinal diseases get more and more common nowadays; e.g., lifetime risk of osteoporotic fracture is 40% for white women and 13% for white men in the United States. Thus the numbers of surgical spinal procedures are also increasing with the aging population and precise diagnosis plays a vital role in reducing complication and recurrence of symptoms. Spinal imaging of vertebral column is a tedious process subjected to interpretation errors. In this contribution, we aim to reduce time and error for vertebral interpretation by applying and studying the GrowCut-algorithm for boundary segmentation between vertebral body compacta and surrounding structures. GrowCut is a competitive region growing algorithm using cellular automata. For our study, vertebral T2-weighted Magnetic Resonance Imaging (MRI) scans were first manually outlined by neurosurgeons. Then, the vertebral bodies were segmented in the medical images by a GrowCut-trained physician using the semi-automated GrowCut-algorithm. Afterwards, results of both segmentation processes were compared using the Dice Similarity Coefficient (DSC) and the Hausdorff Distance (HD). In addition, the times have been measured during the manual and the GrowCut segmentations, showing that a GrowCut-segmentation – with an average time of less than six minutes (5.77±0.73) – is significantly shorter than a pure manual outlining.

Methods

Similar to[1-3] for glioblastoma multiforme (GBM)[4,5], Pituitary Adenoma[6] and lung cancer the software used during this study for the semi-automatic segmentation work was Slicer (www.slicer.org)[7,8]. Thus, the following step-by-step workflow to perform vertebral body segmentation has been used:

-loading the patient dataset into the Slicer Platform;

-initializing the foreground and background for GrowCut, by marking an area inside and around the identified vertebral bodies;

-running the automatic competing region-growing in Slicer; and

-using morphological operations like dilation, erosion, and island removal for post-editing after visual inspection of the results.

Briefly, GrowCut is a competitive region-growing algorithm using cellular automata that uses an iterative labeling procedure. Figure 1 shows a L4 vertebra after the dataset is loaded with a typical user initialization for GrowCut on the axial, sagittal and coronal cross-sections on the right side.

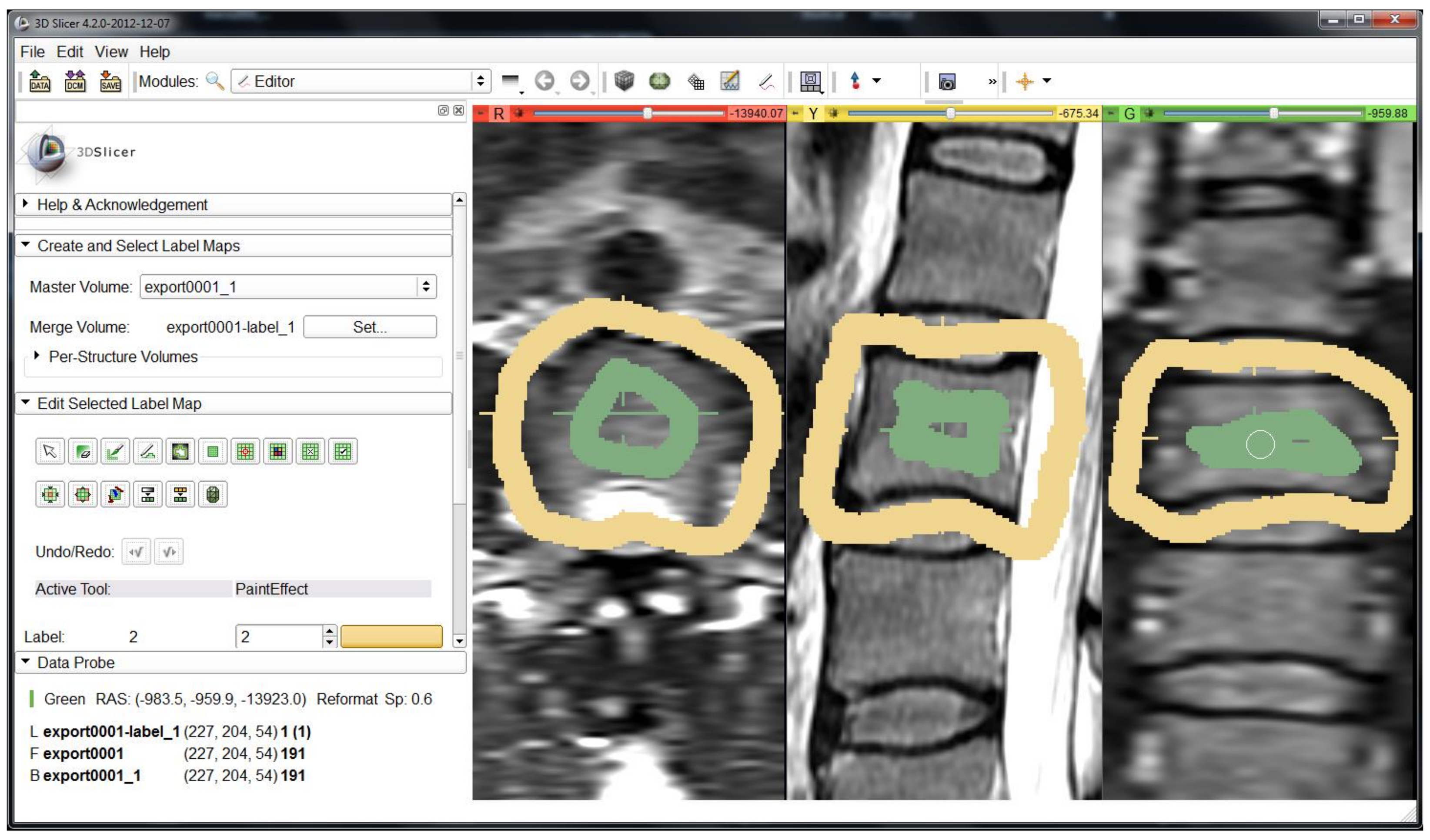

Figure 1 – Typical user initialization of GrowCut.

Results

As comparison metrics for our study, the GrowCut-based vertebral body segmentation results have been evaluated against manually slice-by-slice segmentations using the Dice Similarity Coefficient (DSC) and the Hausdorff Distance (HD). The DSC is a measure for spatial overlap of different segmentation results, which is commonly used in medical imaging studies to quantify the degree of overlap between two segmented objects A and R:

$$DSC = \frac{2 \cdot V(A \cap R)}{V(A) + V(R)}$$

Thereby, the DSC can have a value ranging from zero to one, and is defined as two times the volume of the intersection between the two segmentations A and R, divided by the sum of the volumes of the two segmentations. A value of zero indicates no overlap and a value of one indicates a perfect agreement, and as a consequence higher values indicate a better agreement. The Hausdorff Distance is used to calculate how far away (in voxel) the two segmentations A and R are. As gold standard to calculate the DSCs and the Hausdorff Distances we had manual segmentations of vertebrae boundaries extracted by several clinical experts (neurological surgeons) with many years of experience in spine surgery. Compared with the GrowCut-based segmentation results from a trained physician we discovered an average Dice Similarity Coefficient of 82.99±5.03% and Hausdorff Distance of 18.91±7.2 voxel. For visual inspection, a direct comparison of a manual (yellow) and a GrowCut-based segmentation (green) on a sagittal slice is presented in Figure 2: the left image shows the original MRI slice, the next image from the left presents the manual segmentation, the third image from the left presents the GrowCut-based segmentation result, and the right image presents both segmentations (manual and GrowCut) superimposed on the original MRI slice.

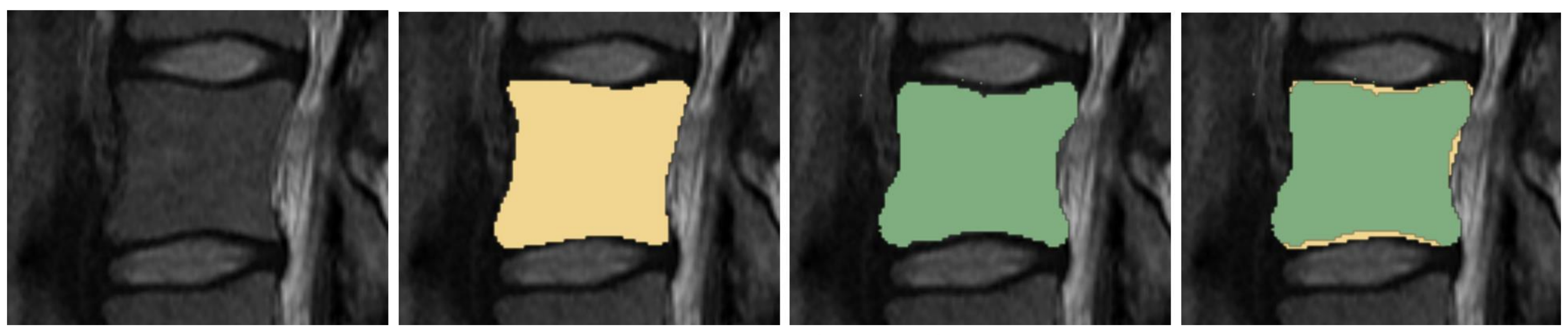

Figure 2 – Direct comparison of a manual (yellow) and the automatic segmentation (green) on a sagittal slice: The left image shows the original MRI slice, the adjacent image presents the manual segmentation, the third image from the left presents the GrowCut segmentation result and the right image presents both segmentations (manual and GrowCut) superimposed on the MRI slice.

Conclusions

In this study, we used the interactive GrowCut algorithm, based on cellular automata, for 3D segmentation of vertebral bodies (note: preliminary results have been presented at the spine congress of the DGNC in Frankfurt, Germany). In summary, we found that a semi-automated segmentation using the GrowCut algorithm reduces segmentation time while at the same time achieves a similar accuracy as pure manual slice-by-slice segmentations. For evaluation of the GrowCut segmentation results, we used vertebrae images from MRI datasets, which have been manually outlined by physicians, and which took in average over ten minutes (10.75±6.65) for a single vertebra in our datasets. There are several areas of future work: The GrowCut algorithm initialization has initially been set up by the user in three slices for this study. However, instead of initializing the foreground and background on three single 2D slices, one single 3D initialization could be used by means of generating a sphere around the position of a user-defined seed point near the center of the vertebral body. Furthermore, we want to test GrowCut on longitudinal/tubular structures, like vessels[9-14] or fiber tracts[15,16].

References

1. Egger, J. et al. "GBM Volumetry using the 3D Slicer Medical Image Computing Platform," Sci Rep. 3; Nature Publishing Group (NPG), DOI:10.1038/srep01364 (2013).
2. Egger, J. et al. "Pituitary Adenoma Volumetry with 3D Slicer," PLOS ONE 7 (12), e51788 (2012).
3. Velazquez, E. R. et al. "Volumetric CT-based segmentation of NSCLC using 3D-Slicer," Sci Rep. 3; Nature Publishing Group (NPG), DOI:10.1038/srep03529 (2013).
4. Egger, J. et al "A flexible semi-automatic approach for glioblastoma multiforme segmentation," Proceedings of International Biosignal Processing Conference, Charité, Berlin, Germany (2010).
5. Egger, J. et al. "Nugget-Cut: A Segmentation Scheme for Spherically- and Elliptically-Shaped 3D Objects," 32nd Annual Symposium of the German Association for Pattern Recognition (DAGM), LNCS 6376, pp. 383-392, Springer Press, Darmstadt, Germany (2010).
6. Egger, J. et al. "Pituitary Adenoma Segmentation," In: Proceedings of International Biosignal Processing Conference, Charité, Berlin, Germany (2010).
7. Kuhnt, D. et al. "Fiber tractography based on diffusion tensor imaging compared with high-angular-resolution diffusion imaging with compressed sensing: initial experience," Neurosurgery, 72, 165-175 (2013).
8. Egger, J. et al. "Integration of the OpenIGTLink Network Protocol for image-guided therapy with the medical platform MeVisLab," Int J Med Robot, 8(3):282-90 (2012).
9. Renapurkara, R. D. et al. "Aortic volume as an indicator of disease progression in patients with untreated infrarenal abdominal aneurysm," European Journal of Radiology 81 (2012) e87–e93 (2012).
10. Egger, J. et al. "A Fast Vessel Centerline Extraction Algorithm for Catheter Simulation," 20th IEEE International Symposium on Computer-Based Medical Systems, Maribor, Slovenia, pp. 177-182, (2007).
11. Lu, J. et al. "Detection and visualization of endoleaks in CT data for monitoring of thoracic and abdominal aortic aneurysm stents," SPIE Med. Imaging, Vol. 6918, pp. 69181F(1-7), San Diego, USA, (2008).
12. Egger, J. et al. "Simulation of bifurcated stent grafts to treat abdominal aortic aneurysms (AAA)," Proceedings of SPIE Medical Imaging Conference, Vol. 6509, pp. 65091N(1-6), San Diego, USA (2007).
13. Egger, J. et al. "Preoperative Measurement of Aneurysms and Stenosis and Stent-Simulation for Endovascular Treatment," IEEE International Symposium on Biomedical Imaging: From Nano to Macro, Washington (D.C.), USA, pp. 392-395, IEEE Press (2007).
14. Greiner, K. et al. "Segmentation of Aortic Aneurysms in CTA Images with the Statistic Approach of the Active Appearance Models," Proceedings of BVM, Berlin, Germany, Springer Press, pages 51-55 (2008).
15. Bauer, M. et al. "Boundary estimation of fiber bundles derived from diffusion tensor images," International journal of computer assisted radiology and surgery 6 (1), 1-11 (2011).
16. Bauer, M. et al. "A fast and robust graph-based approach for boundary estimation of fiber bundles relying on fractional anisotropy maps," 20th ICPR, Istanbul, Turkey, pp. 4016-4019 (2010).

SPIE. MEDICAL IMAGING

Town & Country Resort and Convention Center
San Diego, CA, United States
27 February - 3 March 2016